# Capacity Recovery and Failure Detection EV Batteries

*Chakib Alaoui, Taif University, KSA.*

***Abstract* -- This work is about the design, implementation and testing of a system for control and management of the energy delivered to and consumed by Electric Vehicle. Low power and high power algorithms were implemented on an FPGA that was installed on an Electric Vehicle. This integrated circuit uses recent battery models, with Rate Capacity effect and Recovery effect to rejuvenate the batteries. This system allows the batteries to recover to more than 90% of their initial capacity without dismantling them nor unloading them from the EV, extends the useful life of the batteries and makes the EV more user-friendlier.**

## I. INTRODUCTION

Concerns over oil dependency, as well as concerns over increasing pollution in major urban areas have caused a resurgence of research activities aimed at developing a practical and dependable Electric or Hybrid Vehicle. Several promising vehicles have been constructed and tested, but battery performance-related obstacles have prevented these vehicles from being practical.

The development of a high-energy battery would be the "break-through" that the EV industry is waiting for. However, most of the existing EVs on the road in the present day use lead-acid batteries. They meet the requirement of inner-city commuters, who need daily driving ranges of only 30-50 miles. Unfortunately, the EV community has found that the typical lead-acid EV batteries often start to perform unreliably after few 10's of cycles in spite of high-quality construction [1]. Sulfation is a very common problem that occurs in this type of batteries. It occurs when lead sulfate cannot be converted back to charged materials and is created when discharged batteries stand for a long time. When the state of charge drops below 80%, the plates become coated with a hard and dense layer of lead sulfate that fills-up the pores. Nickel-cadmium and nickel metal hydride batteries are used for longer driving ranges (<150 miles), but like the lead acid, they are affected by battery-voltage imbalance within the pack, high/low temperature effect, memory effects, self-discharge and internal impedance imbalance [2]. Maintaining an optimum and uniform battery capacities of the whole pack is a key solution to maintain the initial EV range for longer time, and extend the batteries useful life.

The variations in temperature and capacities among individual batteries connected in series lead to imbalance with regards to the state of degradation of each battery. In addition, cells having higher rate degradation tend to over-discharge relative to the other cells, which further aggravate degradation in an endless cycle. Moreover, gas recombination reaction during charging acts to unbalance the state of charge among the cells. Slightly degraded cells have high internal resistance and therefore a high rise in voltage during charging, which excessively generates electrolysis and decreases of water in process. There have been many techniques aimed to improve the life cycle of the EV batteries [3-6].

Additionally, the rates of charge and discharge play an important role on the battery's lifetime. When the discharge current is low, the inactive sites are distributed uniformly throughout the cathode. However at higher discharge rates, the chemical reactions occur at the outer surface of the cathode making the inner active sites passive. As a consequence, the energy delivered decreases. This phenomenon is called Rate Capacity Effect [7]. This effect can be significantly reduced by having a pulsed discharge current instead of constant current. This allows the cell to relax after delivering a current. The diffusion process compensates for the depletion of active materials that takes place during the current drain. This is called Recovery effect, or Relaxation Effect [8]. Several battery models were presented in the literature, a Spice model was presented in [9-10]. Batteries were also modelled using electrochemical models [11]. In this paper, analytical battery models will be used.

Cell balancing techniques have been discussed in several publications [12-13]. Multiple-cell Lead-Acid battery packs are sometimes equalized by a technique known as 'controlled-overcharge'. These techniques eliminate the need to periodically adjust individual cells to match the rest of the pack.

1. Charge Shunting: selectively shunts the charging current around each cell as they become fully charged. This method lacks of efficiency because resistor are used to shunt cells, and the current is dissipated through the Joule effect. Hence this method is unsuitable due to the large currents in EVs.
2. Charge-Shuttling: Charge shuttling cell balancing mechanisms consist of a device that removes charge from a selected cell, stores that charge, and then delivers it to another cell. Usually, 'flying capacitors' are used as storage elements. This method is also unsuitable for the large EV batteries, since the capacitance values and the resistance due to switching losses would dramatically

increase the time constant. A large (100Ahr) battery pack would require a charge shuttling device with a very large capacitor with extremely large switch currents.

3. Energy Converters: Cell balancing utilizing energy conversion devices employs inductors or transformers to move energy from a cell or group of cells to another cell or group of cells. This method has been used in this paper because of the small size and the high efficiency of electronic devices.

There have been also numerous patents of systems dealing with battery management systems for EVs and other applications [15-16]. There have been also many attempts to manage and optimize the energy consumed by Electric and Hybrid Vehicles, from a mechanical perspective: [17] describes a control on a "Continuous Variable Transmission (CVT)" that offers fuel and battery charge economies. This solution deals with the mechanical aspect of the vehicles. [18] is another mechanical optimization of the energy used by the motors. The system is able to diagnose faults in the motors, controllers or the batteries, and change gears according to the desired speed having the best energy utilization. And from electrical perspective: [19] describes three strategies on how to operate Hybrid vehicles efficiently by using off-board electricity generation to recharge their batteries. But this solution works for Hybrid Vehicles only. [20] Describes how Fuel-cells and Super-Capacitors can be utilized to increase the driving range of the electric Vehicles, increase battery life and energy economy. But this solution makes the Electric Vehicles more expensive due to the additional costs.

There has never been an attempt to apply the rejuvenation algorithms to electric car batteries without dismantling the batteries. The capacity loss and the battery unbalance within the EV are unresolved issues in EVs so far.

This paper shows algorithms for diagnostic and rejuvenation of Electric Vehicle batteries implemented on a reconfigurable System-on-Chip. Once installed on the vehicle, this system has three main functions:

1. Acquire individual battery voltage and temperature when the vehicle is on the road,
2. Apply the low power rejuvenation algorithm when the vehicle is stationary and plugged at a residential power source (220/110V~ 50/60Hz)
3. Apply high power rejuvenation algorithm when the vehicle is connected to a high power source, in an electric vehicle service station as example. This system will keep similar capacities within the battery pack; it will extend the useful life of all the batteries within the electric vehicle.

## II. BATTERY MODELS

### A. Discharge Rate Dependent Model

Discharge rate dependent model considers the effect of battery discharge rate on the maximum capacity (1). [21] Showed that battery's capacity is reduced as the discharge rate increases.

$$C = k.C_0 - \int i(t)\,dt \qquad (1)$$

$$k = C_{eff}/C_{max}$$

Where ***Ceff*** is the effective battery capacity and ***Cmax*** is the maximum capacity of the battery. ***k*** is the battery capacity efficiency factor.

The factor ***k*** can be obtained from the battery manufacturer datasheet that shows ***Ceff*** versus ***i(t)***. Then the remaining capacity can be commuted. Typical values of k approach 0 when the discharge current is high and approach 1 when the discharge current is low. This behaviour shows the rate capacity effect, but it does not portray the recovery effect.

### B. Stochastic Kinetic Battery Model (Recovery Model)

The relaxation model (also called Stochastic Battery Model and Relaxation model) [22] focuses on the Recovery effect and models the battery behaviour as Markov process with probabilities related to the physical characteristics of the electrochemical battery cell. This model is the most comprehensive and the closer to the real battery, however it is the most difficult to implement. Some stochastic models have been reported in the literature, e.g. a discrete time VHDL model [23], and a discrete time Markovian chain model [24] that includes the recovery model. The battery is modelled as two wells of charge, as shown in Figure 1 [25].

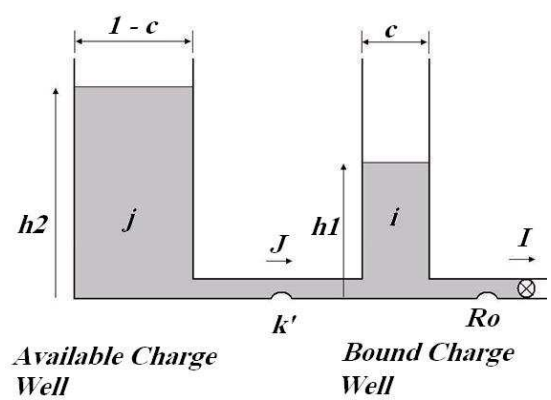


Fig. 1. Stochastic Kinetic Battery Model

The bound charge well supplies electrons directly to the load; the available charge well supplies electrons to the bound charge well. Refer to equation (2).

$$i = h1.c$$

$$j = h2.(1 - c) \qquad (2)$$

Where ***c*** is the capacity ratio, corresponds to the effective total charge. ***i*** is the amount of charge in the bound charge well, and ***j*** is the amount of charge in the available charge well. ***k'*** is the rate of charge flow between the two wells. ***Ro*** is

the internal resistance of the battery, it limits the output current I. The rate of transfer between the two wells is expressed in equation (3).

$$j = k' \cdot h_2 \cdot (h_2 - h_1) \qquad (3)$$

The present work shows the design, implementation and testing of low-power and high-power algorithms that takes into account the Capacity and Recovery Effects.

## III. EXPERIMENTAL SYSTEM DESCRIPTION

### *A. The Electric Vehicle*

The system was designed to fit Solectria Electric Vehicle of type "force". This vehicle was manufactured by Solectria Corporation [26]. The following are some specifications:

- Conversion of Geo Metro of 1992
- Seating Capacity: 2 Adults
- Front Wheel Drive
- Range: 50 to 60 miles
- Maximum Speed: 65 miles per hour
- 12 batteries of type Hawker 12 Volts, 38AH
- Motor: AC Induction

5 of the 12 batteries are located in the front battery box, and the 7 remaining are located in the rear box in order to have an even weight distribution. This electric vehicle comes equipped with a charger of 1.5KW. This charger will be used for the low power rejuvenation algorithm. This vehicle has also two standard electric resistance heaters in the passenger compartment and a small conventional air conditioner. The system has a compressor/motor combination, a motor controller, a condenser, a fan, an evaporator and a hose system. The compressor/motor combination is located on the top of the front battery compartment, which makes it difficult to service the batteries.

### *B. Rejuvenation System*

This system is composed by three units:

1. Voltage and temperature acquisition unit
2. Low power rejuvenation unit
3. High power rejuvenation unit

These units are controlled by an FPGA Chip where all the algorithms were implemented. Figure 2 shows the block diagram of the system.

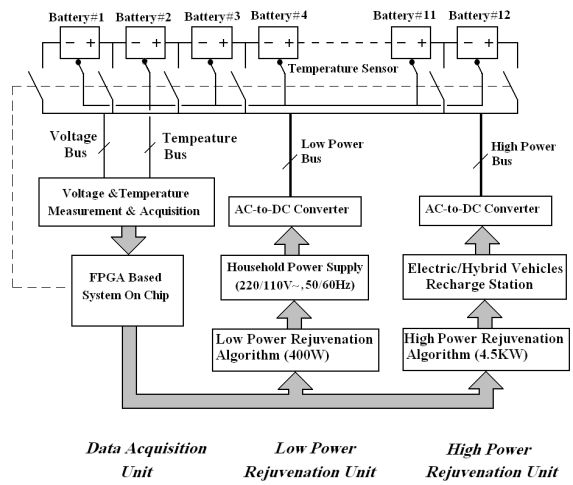


Fig. 2. Block diagram for the system for energy control & management for EVs and HVs. The SoC acquires the voltage and temperature measurements, applies the low power rejuvenation algorithm or the high power rejuvenation algorithm.

This system is controlled by the FPGA solution Virtex XCV800 of Xilinx. This solution was chosen because of its numerous attributes, mainly its capability of implementing high performance System-On-Chip designs previously the exclusive domain of custom ASICs (Application Specific ICs), yet with the flexibility and low development cost of programmable logic. It has some advantages over the microprocessors, where all the functions are implemented as software. FPGA offers the advantage of 'hardwiring' the functions. Complex user-defined system architectures can be easily synthesized through a programming language like the VHDL, which produces a "configuration file", used to configure the FPGA. This solution is used in many industrial applications such as signal processing, industrial control, image processing, networking, communications, and aeronautic applications [27]. Figure 3 shows the input and output signals of the FPGA.

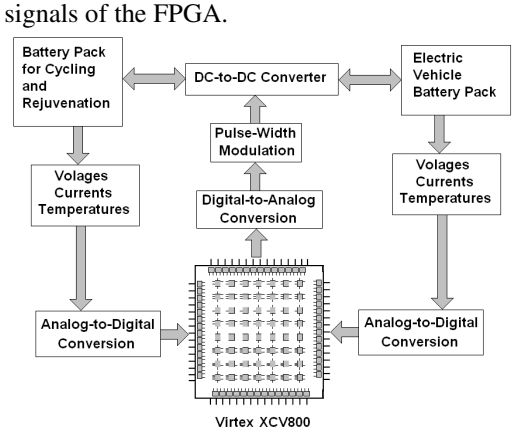


Fig. 3. Virtex XCV800 bloc diagram. Its inputs are the battery voltages, currents and temperatures, and ambient temperature. Its output is sent to a pulse-width modulator to control the DC-to-DC converter.

First, the rejuvenation algorithms were developed and implemented in a regular computer by using high level

language C. Once the algorithm is verified, it is then implemented on the FPGA chip by using a hardware description language VHDL. Table 1 shows the available resources in Virtex.

TABLE I
RESOURCES AVAILABLE IN VIRTEX XCV800

| | |
|---|---|
| System Gates | 888,440 |
| Total Configurable Logic Blocks | 4704 |
| Maximum User Input/Output | 240 |

The design procedure of the FPGA chip was of five basic steps: design entry, simulation, synthesis, implementation and device download/program file formatting. This was done thank to the Xilinx ISE 6.1 CAD tool package.

The following shows the implementation results:

- Number of slices: 5930 out of 9408 (63%)
- Number of Slice Flip-Flops: 9220 out of 18816 (49%)
- Number of Look-up-Tables (4 inputs): 137 out of 170 (80%)
- Number of Bonded Input/Output Blocks: 110 out of 170 (65%)

## IV. HIGH POWER/LOW POWER REJUVENATION ALGORITHMS

### *A. High Power Hardware Design*

When high power is available, as in a charging station for electric & hybrid vehicles, the vehicle's batteries may be rejuvenated according to the high power algorithm. It applies to or sinks from the batteries a maximum current of 25 A (as specified from the battery manufacturer) in order to cycle them. (1 cycle = 1 full charge + 1 full discharge).

Figure 4 shows the hardware set-up for this rejuvenation algorithm. An external battery pack was used in the charging station in order to cycle the batteries. This solution was chosen because of the following advantages:

- The batteries are capable to deliver high power in a short-time. This is needed when applying the high power rejuvenation algorithm.
- When charging and discharging the EV batteries through the external battery pack, the energy is not totally wasted. About 85% of the energy is 'recycled' (the batteries are about 80% efficient and the DC-to-DC converter is more than 90% efficient).

A DC-to-DC converter of type "buck-boost" [28] was designed to transfer back-and-forth the unregulated dc power coming from a bulk batteries of 216 Volts (3 parallel sets of 18 12 Volts batteries) into the Electric Vehicle. The EV has 12x12 Volts batteries.

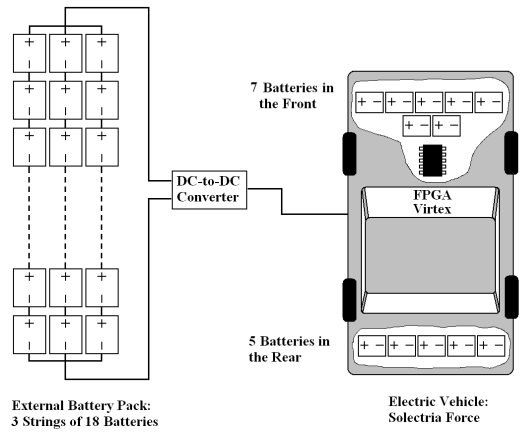


Fig. 4. High power rejuvenation set-up. An external battery pack made of 3 strings of 18 batteries connected en series serve to rejuvenate the EV batteries by cycling them according to the high power rejuvenation algorithm

### *B. High Power Charge/Discharge Methodology*

Many types of charging/discharging algorithms have been developed in past decade, and they all have some advantages/disadvantages associated with each one of them:

1. Some early commercial chargers employed constant current charging for a preset duration. The efficiency of this type of charger is low since the state of charge is not taken into account. Even with low initial state of charge, the battery may be evolving gas significantly in the last quarter of the charging cycle [9-12].
2. Constant voltage charging technique is also very popular and convenient, but it leads to undercharging since it takes 'infinite' time to charge the battery completely by this method since the charging current decreases asymptotically.
3. Taper charging algorithm, that combines both techniques, has been used in this project. The EV batteries are first supplied with a constant charging current until the battery pack approaches the voltage limit (15 Volts/unit on average with corresponds to gas evolution specified by the battery manufacturer). Then, the charging current is decreased until the voltage limit (15 Volts/battery) is finally reached.

Concerning the discharge, continuous and intermittent discharge current values have been applied in order to allow the Recovery Effect of the EV batteries. This results in an increased service life [9-12]. This improvement is generally greater at the higher current drains, as the battery has the opportunity to recover from the polarization effects that have more pronounced effects at the heavier loads.

The high-power rejuvenation algorithm can be described by the following steps:

1. First, they are discharged at a constant current of 20 Amps (value proposed by the battery manufacturer)
2. As soon as any battery reaches 10.5 Volts (lower limit imposed by the manufacturer); the discharge current is then reduced by 5 Amps. It should be noticed that at that

time, the battery voltages increase thanks to the recovery effect described in section II.

3. This technique is repeated until the discharge current is less than 5 Amps. Then the batteries are discharged by the low rate of 1 Amps during at least 5 hours.

Finally the batteries are charged. At this stage, the input charge to the EV shows that the batteries are recuperating some of their lost capacity. Figure 6 shows the rejuvenating algorithms.

### *C. Low Power Hardware Design*

When the vehicle is off-road for several hours, especially overnight, it is possible to apply the low power rejuvenation algorithm to it, given that a household low power is available. This system applies a technique that is similar to the 'cell balancing technique' described in [14], but will be applied to individual batteries instead of individual cells.

This system will start by checking the state of charge of the whole battery pack. If the total voltage is less than 144 Volts, which corresponds to an average of 12Volts for each battery, then the system will apply an input power of 1.5KW to the whole pack until it brings the total voltage to 144V. Then it will recharge individual batteries, according to their state of charge. The algorithm will use the data recorded while the vehicle was on the road to identify any battery(s) having a lower voltage than average, and then will bring its state of charge equal to the average. The same will be done to the next battery having the lowest voltage and so on until the whole pack is rejuvenated. Figure 5 shows the control circuit for the low power, and figure 6 shows the rejuvenation algorithm.

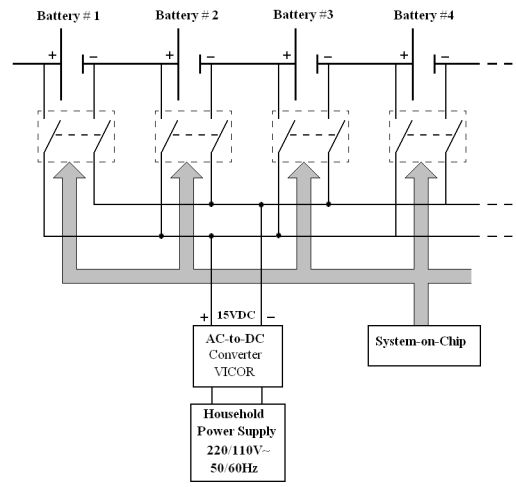


Fig.5. Control circuit for low power rejuvenation algorithm

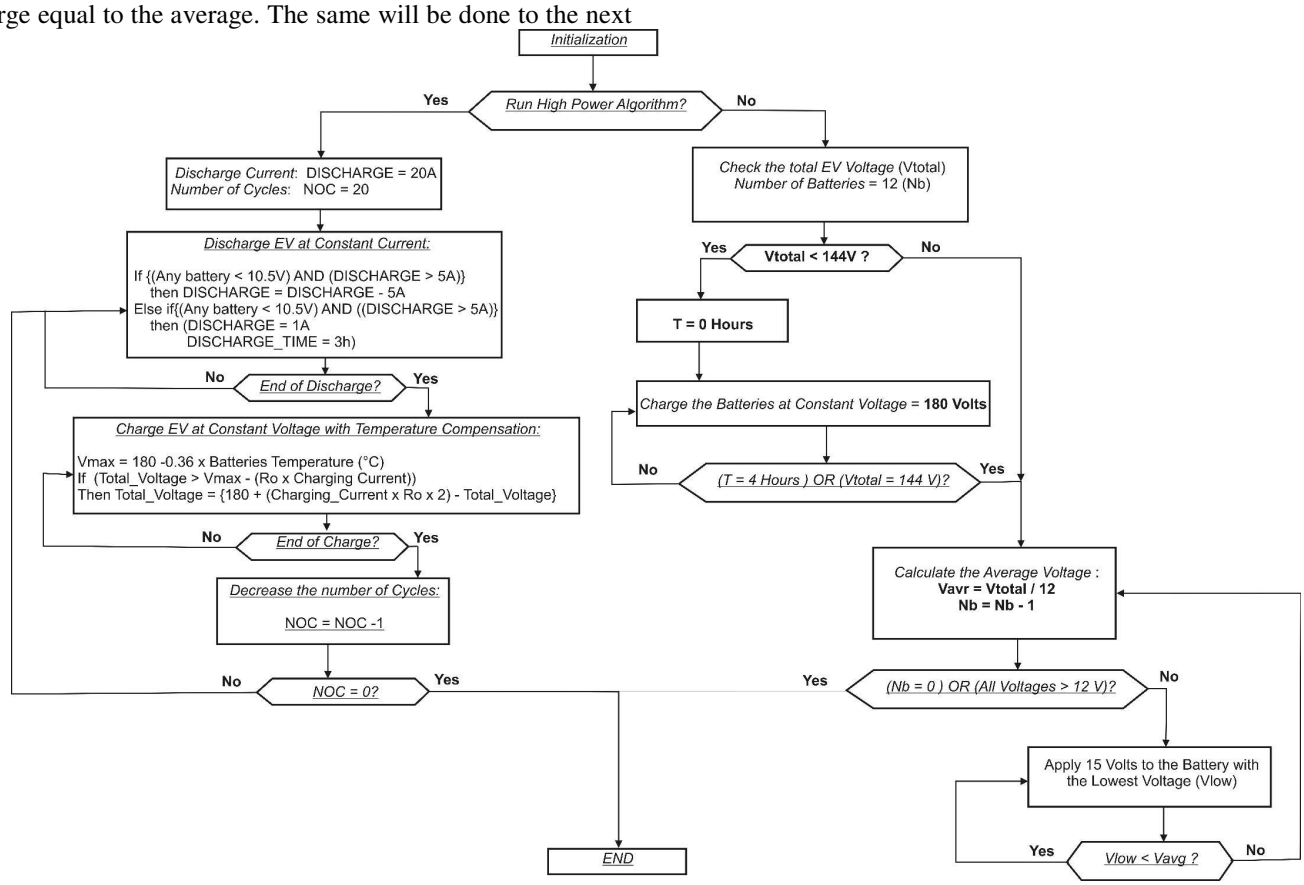


Fig.6. Rejuvenating Algorithms

## V. EXPERIMENTAL RESULTS

### *A. High Power Rejuvenation Algorithm*

12 used sealed lead acid batteries for EVs were picked randomly and installed in the Electric Vehicle. These batteries were rated at 38 AH, but had different states of charge. While a load was applied, a first quick check on their voltages is shown in table 2. This diagnostic indicates that the batteries have different state of charge. The battery number 11 has the worst voltage (9.5 Volts) and consequently will be the first to fail within the pack if the EV is not rejuvenated.

TABLE 2
EV BATTERY VOLTAGES BEFORE AND AFTER HIGH POWER REJUVENATION

| Battery Number | Before Rejuvenation | After Rejuvenation |
|---|---|---|
| 1 | 11.5 | 12.87 |
| 2 | 11.7 | 12.68 |
| 3 | 11.01 | 12.55 |
| 4 | 12.08 | 12.43 |
| 5 | 11.95 | 12.47 |
| 6 | 12.53 | 12.62 |
| 7 | 11.53 | 12.55 |
| 8 | 10.02 | 12.45 |
| 9 | 10.95 | 12.39 |
| 10 | 10.54 | 12.59 |
| 11 | • 9.5 | 12.66 |
| 12 | 11.12 | 12.65 |

Before rejuvenation, the EV pack has an average voltage of 11.20 Volts. It should be noted that in the ideal case, the individual battery voltages must be as close as possible to the average voltage. The capacity of the EV battery pack was also evaluated. It should be also noted that because of the series connection of the batteries, the range of the EV is determined by the smallest battery capacity within the pack.

After a full discharge followed by a full charge, the capacity of the EV pack was computed according to the battery linear model, by using equation (5).

$$C = \int i \, . \, dt \qquad (5)$$

Where $\boldsymbol{C}$ is the capacity (AH) and $\boldsymbol{i}$ is the current (A). The initial capacity was 22 Ampere-Hours.

The EV pack was discharged following the algorithm described before. Figure 7 and Figure 8 show the total voltage and the current.

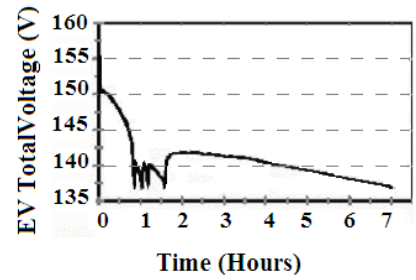


Fig. 7. EV Battery Pack Voltage during discharge.

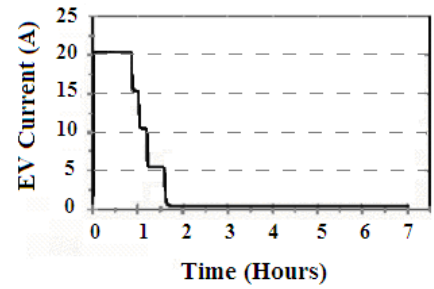


Fig. 8. Discharge Current in EV battery pack.

Figure 7 shows a starting discharge current of 20 A. About 50 minutes later, the battery #11 had its voltage dropping to 10.5V. The discharging current was then dropped to 15A. A voltage recovery is then noticed to 141V. This technique was repeated for 10A and 5A. Finally, a constant discharge current of 0.5A was applied for 5 hours.

The EV pack was charged according to the charging algorithm described in Figure 7 (Refer to Figure 9 and Figure 10). First, the batteries were charged at constant current until the batteries voltage limit was approached (15Volts average x 12 = 180), then the current decreases until the end of charge.

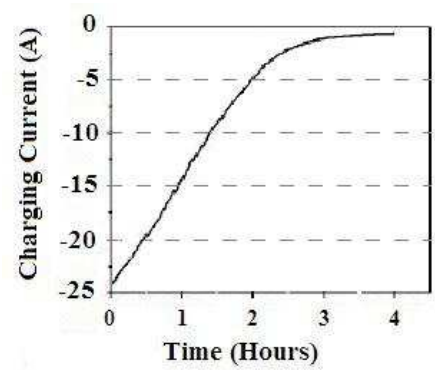


Fig. 9. Charging Current in EV battery Pack.

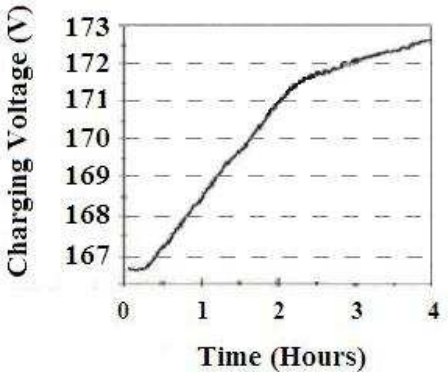

Fig. 10. Charging Voltage in EV battery pack.

This charge by voltage-limit was temperature compensated according to relationship (6) specified by the battery manufacturer:

Maximum applicable voltage = 180 – 0.36 x Temperature (ºC) (6)

The prescribed rejuvenation algorithm was followed and the batteries were rejuvenated. After 5 cycles following the same procedure, the capacity of the string of batteries was measured. It rose to 36.5 AH, which was close to the initial capacity of 38 AH. Also the average battery voltage was 12.59Volts, and all individual battery voltages felt within 5% of the average.

This rejuvenation algorithm allows the application of the highest voltage on the batteries in order to break down the hard lead sulfate crystals, while staying within the voltage range specified by the manufacturer (10.5Volts to 15 Volts).

*B. Low power rejuvenation algorithm*

A set of 12 batteries with different states of charge were mounted on the vehicle, and the low power rejuvenation algorithm was run. Table 3 shows the individual battery voltages before and after rejuvenation.

TABLE 3
EV BATTERY VOLTAGES BEFORE AND AFTER LOW POWER REJUVENATION

| Battery Number | Before Rejuvenation | After Rejuvenation |
|---|---|---|
| 1 | 11.40 | 12.44 |
| 2 | 11.98 | 12.83 |
| 3 | • 10.37 | 12.12 |
| 4 | 11.69 | 12.69 |
| 5 | 11.09 | 12.09 |
| 6 | • 9.67 | 12.03 |
| 7 | 11.07 | 12.08 |
| 8 | • 9.74 | 12.12 |
| 9 | 10.53 | 12.19 |
| 10 | 11.10 | 12.19 |
| 11 | 11.06 | 12.08 |
| 12 | 11.48 | 12.52 |

The batteries were initially at different levels of discharge. Moreover the batteries numbered 6 and 8 have the lowest voltages. The initial total voltage is 131.18 Volts. The electric vehicle is equipped with a charger that was set-up to give a constant voltage to the batteries (12X15V=180V). This charger is controlled by the FPGA chip Virtex, which runs the low-power rejuvenation algorithm. The initial total battery voltage was 131.18Volts and was raised to 144.38Volts after 105 minutes as shown in Figure 11.

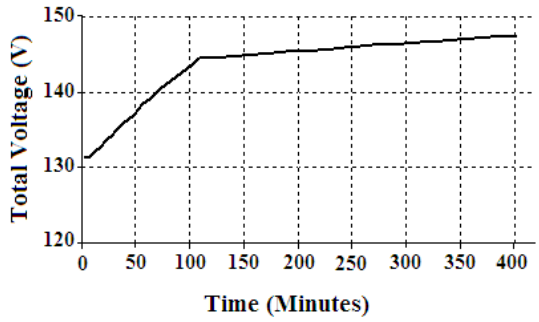

Fig. 11. Total battery voltages. It took more than 6 hours to run the low power rejuvenation algorithm

After 105 minutes, the main charger of the vehicle was disconnected, and a small charger was connected to battery 6 that had the lowest voltage of 11.04Volts. It took an additional 100 minutes to raise its voltage to the average which was of 144.38Volts/12 = 12.03 Volts. Figure 12 shows individual battery voltages. It shows that initially, the battery voltages were very different as they were between 9.6 V and 12V. But after the application of the rejuvenation algorithm, the battery pack became more compatible (12.05V to 12.74V).

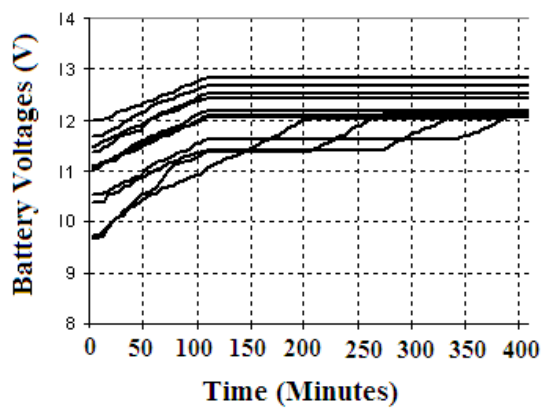

Fig. 12. After about 400 minutes, the 12 battery voltages converge to values between 12.1 and 12.8 Volts.

## VI. CONCLUSIONS

Battery-powered electric vehicles need efficient battery rejuvenation in order to increase battery life. In this paper, an overview of battery models was given. Then rejuvenating

algorithms that take advantage of the 'Recovery model' were implemented on a system-on-chip and tested. Experimental results show that, for high power, taper algorithm for charging, combined with continuous and intermittent current values for discharging, as described in section V-b, have shown improvement in battery capacities (From 22 to 36.5 AH). Concerning low power rejuvenation, this system applies a technique that is similar to the 'cell balancing technique' described in [14], but will be applied to individual batteries instead of individual cells. The experimental results show more balanced and compatible battery voltages.

Additional practical benefits include the identification of 'weak' battery and its rejuvenation without dismantling the vehicle. The user has to choice of running the high power rejuvenation or the low power rejuvenation algorithms pending on the power available (Household power supply or high power recharge station). It is recommended to run the high power rejuvenation algorithm described in this paper periodically (every 2 – 3 months) in order to maximize the productive life of the Electric Vehicle batteries.

REFERENCES


[1] C. Alaoui, Z. M. Salameh, "Experiments in fast charging lead acid electric vehicle batteries", *Vehicular Technology Conference*, VTC 2003.

[2] E. Jelinski, P. Olsen, "Design, Manufacturing and Operating Experience with an Electric Vehicle: Cold Climate Experience". *Society of Automotive Engineers*, March 1997.

[3] M. Origuchi, T. Miyamoto, H. Horie, K. Katayama, "Development of a Lithium-ion Battery System for EVs". *SAE International*. Ref. 970238.

[4] T. Palanisamy "Charging Techniques for a universal Lead-Acid Battery Charger", Corporate Research and Technology Allied-Signal, Inc., 1995

[5] M. J. Riezenman, "The Search for Better Batteries", *IEEE Spectrum*, May 1995.

[6] C. Toepfer, "Charge! EVs Power-Up for the Long Haul", *IEEE Spectrum*, November 1998.

[7] M. Doyle, J. S. Newman, "Analysis of capacity-rate data for lithium batteries using simplified models of the discharge process." *J. Applied Electrochemistry*, pp. 846-856, July 1997.

[8] T. L. Martin, "Balancing Batteries, Power and Performance: System Issues in CPU Speed-Setting for Mobile Computing.", Ph.D thesis, Carnegie Mellon University, Pittsburgh, Pennsylvania, 1999.

[9] S. Gold, "A PSPICE Macromodel for lithium-ion batteries.", *In Proceedings of the 12th Annual Battery Conference on Applications and Advances*, pp. 215-222, January 1997.

[10] S. C. Hageman, "Simple PSpice models let you simulate common battery types," Elec-
tronic Design News, vol. 38, pp. 117 – 129, 1993.

[11] S. Li, J. Evans, "Electrochemical Thermal Model of Lithium Polymer Batteries.", *Journal of Electrochem. Society, Vol. 147*, pp. 2086-2095, June 2000.

[12] Keyser, M., A. Pesaran, M. Mihalic, "Charging Algorithms for Increasing Lead Acid Battery Cycle Life for Electric Vehicles", *the 17th International Electric Vehicle Symposium* (EVS-17), Montreal, Canada, 2000.

[13] E. Sexton, "Improved Charge Algorithms for Valve Regulated Lead Acid Batteries," IEEE 00TH8490, *in Proceedings of the 15 th Annual Battery Conference on Applications and Advances*, Long Beach, California, January 11-14, 1999, 211-216.

[14] S. W. Moore, P. J. Schneider, "A Review of Cell Equalization Methods for Lithium Ion and Lithium Polymer Battery Systems", *Society of Automotive Engineers*, 2001-01-0959

[15] S. Okubo, M. L. Kuang, "Charge Depleting Energy Management Strategy for Plug-In Hybrid Electric Vehicles", Patent No. US 2009/0150015 A1

[16] M. Brulhardt, C. Terrier, "Electric Battery Management Device", Patent No. US00573966A

[17] P. Bowls, H. Peng, X. Zhang, "Energy Management in a Parallel Hybrid Electric Vehicle with a continuously variable transmission", Proceedings of the American Control Conference. Chicago Illinois, June 2000.

[18] J. T. Papadimitropoulos, T. G. Chondros, S. D. Panteliou, "Expert System for Energy Management of Electric Cars", Society of Automotive Engineers, January 1999.

[19] J. Gonder, T. Markel, Energy Management Strategies for Plug-In Hybrid Electric Vehicles", SAE World Congress, April 16-19 2007. Detroit, Michigan

[20] E. Faggioli, P. Rena, V. Danel, "Supercapacitors for the energy management of electric Vehicles", Journal of Power Sources, Vol 84, Issue 2, December 1999. Pages 261-269

[21] D. Linden, "Handbook of Batteries and Fuel Cells", 1984, McGraw-Hill Book Company, New York NY, pp. 67-69.

[22] D. Panigrahi, C. Chiasserini, S. Dey, R. Rao, A. Raghunathan, K. Lahiri, "Battery Life Estimation of Mobile Embedded systems.", *In Proceedings of International Conference on VLSI Design,* pp. 55-63, January 2001.

[23] L. Benini, G. Castelli, A. Macii, M. Poncino and R. Scarci, "A discrete-time battery model for high level power estimation.", *In Proceedings of Design, Automation and Test in Europe*. 2000.

[24] C. F. Chiasserini, Ramesh R. Rao, "Energy Efficient Battery Management.", *IEEE Journal of selected areas in communications*, Vol. 19, N. 7, July 2001.

[25] V. Rao, G. Singhal, A. Kumar, N. Navet, "Battery Model for Embedded Systems.", *Proceedings of the 18th International Conference on VLSI Design*, 2005

[26] AZURE DYNAMICS http://www.azuredynamics.com/fleet_sales.htm, DS5-90 Drive Systems.

[27] XILINX http://www.xilinx.com/products/silicon_solutions/fpgas/virtex/virtex4/

[28] AN2389, "An MCU Based low cost non-inverting buck-boost converter for battery chargers". STMicroelectronics, August 2007.

[29] HARRIS http://www.digchip.com/datasheets/parts/datasheet/235/MCTV75P60E1.php